PERGAMON

Scripta mater. 44 (2001) 847–852

Scripta MATERIALIA

www.elsevier.com/locate/scriptamat

TIME-TEMPERATURE-TRANSFORMATION DIAGRAMS FOR THE GROWTH AND DISSOLUTION OF INCLUSIONS IN LIQUID STEELS

T. Hong and T. DebRoy

Department of Materials Science and Engineering, The Pennsylvania State University, University Park, PA 16802, USA

(Received September 15, 2000)
(Accepted October 9, 2000)

Keywords: Inclusion; Growth; Dissolution; TTT diagram

Introduction

Several aspects of inclusion formation, growth and dissolution in liquid steels have been well studied. These include the thermodynamic stability and diffusion controlled growth and dissolution rates of inclusions [1,2]. By contrast, synthesis of the accumulated knowledge of these component processes has been largely overlooked. Examples in contemporary physical metallurgy indicate that such synthesis can be very useful. For example, the *t*ime-*t*emperature-*t*ransformation (TTT) diagram has become an essential tool to understand phase transformation in alloys. Currently no such unified approach is available for understanding the growth and dissolution behavior of inclusions in liquid steels.

The goal of this paper is to synthesize our current knowledge of stability and growth/dissolution kinetics of inclusions in liquid steels in a form that allows a clear understanding of their growth and dissolution behavior. In particular, a formalism is presented here that describes the effects of time and temperature on the diffusion controlled growth and dissolution kinetics of inclusions in steels of known compositions.

Background

The rates of growth and dissolution of inclusions in liquid steels are calculated based on the following assumptions in order to simplify calculations:

1. The concentration field near each inclusion was assumed to be constant during the growth or dissolution of inclusions.
2. The activities of liquid iron and all solid compounds were assumed to be unity.
3. At the interface between the inclusion and the liquid steel, only the concentrations of those elements that constitute the inclusion were calculated. The concentrations of all other elements were assumed to be the same as those in the bulk metal.
4. The growth and dissolution of inclusions were assumed to be controlled by the diffusion of non-metallic elements of inclusions in liquid steels.

The following reaction is considered at the interface between an inclusion particle and liquid steel:

PII: S1359-6462(00)00675-8

TABLE 1
Standard Free Energy Change for Various Reactions [7,8]
$\Delta G° = a + bT$, kJ/mole

Reaction	a	b
$2\underline{Al} + 3\underline{O} = Al_2O_3$	−1209	0.391
$3\underline{Ti} + 5\underline{O} = Ti_3O_5$	−1756	0.571
$\underline{Ti} + 2\underline{O} = TiO_2$	−675.6	0.234
$\underline{Si} + 2\underline{O} = SiO_2$	−589.7	0.229
$\underline{Mn} + \underline{O} = MnO$	−287.9	0.125
$\underline{Ti} + \underline{N} = TiN$	−338.2	0.104
$\underline{Mn} + 2\underline{Al} + 4\underline{O} = MnO.Al_2O_3$	−1545	0.524
$\underline{Si} + 2\underline{Al} + 5\underline{O} = SiO_2.Al_2O_3$	−1338	0.407
$\underline{Mn} + \underline{Si} + 4\underline{O} = MnO.SiO_2$	−838.8	0.314

The standard state for the solutes is hypothetical 1 wt% solution in iron.

$$xM + yQ \rightleftharpoons M_xQ_y \tag{1}$$

where M is a metallic element such as Al, Ni, Mn, Si or Ti, and Q stands for a nonmetallic element, such as O, N, or S. The equilibrium constant for the reaction is given by equation (2).

$$k_{eq} = \frac{a_{M_xQ_y}}{a_M^x a_Q^y} = \frac{1}{[f_M c_M^i]^x [f_Q c_Q^i]^y} = e^{-\frac{\Delta G^0}{RT}} \tag{2}$$

where $a_{M_x}Q_y$, a_M, and a_Q are the activities of M_xQ_y, M and Q, c_M^i and c_Q^i are the interfacial concentrations of M and Q in weight percent, f_M and f_Q are the activity coefficients of M and Q, and ΔG^0 is the standard free energy change for the reaction (1). Considering the ratio of the fluxes of M and Q, the following equation can be derived [3]:

$$c_M^i = c_M^b - \frac{xm_M}{ym_Q}\sqrt{\frac{D_Q}{D_M}}(c_Q^b - c_Q^i) \tag{3}$$

where c_M^b and c_Q^b are the concentrations of M and Q in weight percent in the bulk metal, m_M and m_Q are the atomic weights of M and Q, and D_M and D_Q are the diffusion coefficients of M and Q in liquid steel. The interfacial concentrations of M and Q, c_M^i and c_Q^i, respectively, can be obtained from the solution of equations (2) and (3). These concentrations are used to calculate diffusion controlled growth and dissolution rates as shown in the following sections.

TTT Diagrams for Growth

After a nucleus of inclusion is formed, its growth is calculated by [4]:

$$r_{i+1} - r_i = \frac{\alpha}{2\sqrt{t}}\Delta t \tag{4}$$

where r_i and r_{i+1} are the inclusion radii before and after the *i*th time step, respectively, Δt is the time step, and α is a growth rate parameter [5] expressed by:

$$\alpha = \sqrt{2D_Q c^*} \tag{5}$$

where D_Q is the diffusion coefficient of Q in liquid steel given by

TABLE 2
Alloy Composition and Diffusion Coefficient of Oxygen [9] Used in the Calculations

Element	C	Si	Mn	Ni	Cr	Ti	Al	N	O	S
wt%	0.06	0.39	1.55	0.2	0.01	0.003	0.016	0.004	0.054	0.020
	$D_Q^{1873K} = 1 \times 10^{-8}$ m^2/s						E = 72.5 kJ/mol			

$$D_Q = D_Q^0 \cdot e^{-\frac{E}{RT}} \tag{6}$$

where D_Q^0 is a temperature-independent pre-exponential and E is the activation energy for diffusion. In equation (5), c* is the dimensionless concentration of Q defined by equation (7):

$$c^* = (c_Q^b - c_Q^i)/(c_Q^p - c_Q^i) \tag{7}$$

where c_Q is the concentration of nonmetallic element in weight percent, the subscripts p, b, and i refer to the inclusion particle, bulk liquid metal and inclusion/steel interface, respectively. The time necessary to increase the inclusion radius to a certain value at different temperatures is calculated to construct the TTT diagrams for the growth of inclusions.

TTT Diagrams for Dissolution

Considering diffusion-controlled precipitation with a quasi-steady state approximation, Whelan [6] derived the following expression for the kinetics of precipitate dissolution:

$$r_{i+1} - r_i = -\frac{k}{2}\left[\frac{D_Q}{r_i} + \sqrt{\frac{D_Q}{\pi t}}\right]\Delta t \tag{8}$$

where r_i and r_{i+1} are the radii of the inclusion before and after the *i*th time step, respectively, t is the dissolution time, Δt is the time step, and k is defined as $k = -2c^*$. The time needed to decrease the particle size to a certain value is calculated from equation (8). The results are used to construct the TTT diagrams for dissolution of inclusions.

The standard free energy data for reactions and the alloy composition considered are presented in Tables 1 and 2, respectively.

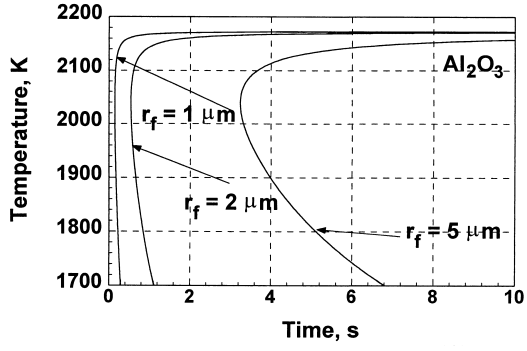

Figure 1. TTT diagrams for the growth of Al_2O_3 inclusions.

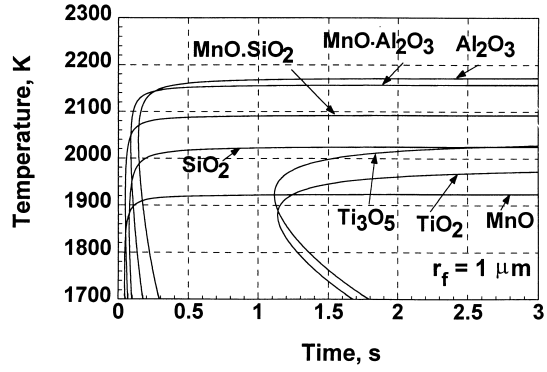

Figure 2. TTT diagrams for the growth of various oxide inclusions.

Results and Discussion

Figure 1 shows the time necessary for Al_2O_3 inclusions to reach various target final radii (r_f) as a function of temperature during isothermal growth. The strong effect of temperature on the growth rate is observed from the figure. When the temperature is above the equilibrium temperature for the inclusion/alloy system, the inclusions will not experience growth. Instead, they will dissolve. It is also observed that the TTT diagrams show the characteristics 'C' shape, i.e., there is a certain temperature where a target size can be attained in a minimum time. The growth rate of inclusions depends on diffusion coefficient, D_Q, and dimensionless supersaturation, c*, as can be observed from equations (4) and (5). When the temperature decreases from the equilibrium temperature for the inclusion/alloy system, the supersaturation increases and the diffusion coefficient decreases. As a result, there is an optimal temperature where the growth rate is fastest.

Figure 2 shows the TTT diagrams for the growth of various oxide inclusions to 1 μm radius. The diagrams for all oxides show the same features observed in Figure 1 for Al_2O_3 inclusions. The stability of the various oxides can be compared with the findings of previous researchers. Kluken and Grong [10] calculated the precipitate stability for a steel of composition considered in this paper. They found that the oxide stability decreased in the following order: Al_2O_3, Ti_3O_5, SiO_2 and MnO. This sequence is same as that indicated from the results in Figure 2. They did not consider any complex oxides. Hsieh *et al.* [11] used ThermoCalc^{TM} to calculate the sequence of oxidation of low alloy steels. Among the

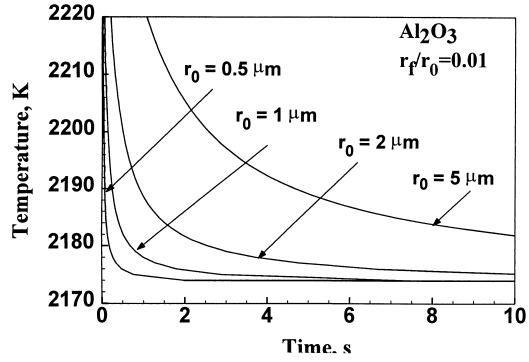

Figure 3. TTT diagram for the dissolution of Al_2O_3 inclusions.

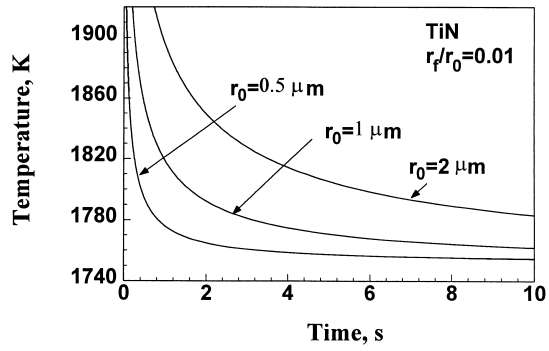

Figure 4. TTT diagrams for the dissolution of TiN inclusion.

oxides considered, Al_2O_3, $MnO{\cdot}Al_2O_3$, and Ti_3O_5 were found to be most stable. Dowling *et al.* [12] studied inclusions in low alloy steel weldments fabricated using submerged arc welding. They found that $MnO{\cdot}Al_2O_3$, a titanium-rich compound, and Al_2O_3 were the main constituents. The high stability of Al_2O_3, $MnO{\cdot}Al_2O_3$ and Ti_3O_5 observed by independent investigators [10–12] is consistent with the computed TTT diagrams presented in Figure 2.

Figure 3 shows the computed TTT diagrams for the dissolution of Al_2O_3 inclusions of different initial radii. It indicates the time necessary to reduce the radii of inclusions from their original radius r_0 to a final radius r_f (1% of r_0 in this plot) at different temperatures. The dissolution kinetics depends strongly on the initial inclusion radius and temperature as can be observed from Figure 3.

Figure 4 shows the TTT diagrams for the dissolution of TiN inclusions of different initial size for an alloy composition indicated in Table 2 but with somewhat higher nitrogen concentration (0.008%). The calculated equilibrium temperature for the TiN/steel system is lower than the melting point of steel of composition indicated in Table 2. However, when the nitrogen concentration is higher (0.008%), the equilibrium temperature is higher than the melting point. The strong effects of time, initial radius, and temperature on the dissolution behavior of TiN are characteristic of all inclusions considered in this investigation.

Concluding Remarks

The effects of time and temperature on the growth and dissolution behavior of inclusions in liquid steel can be represented by a set of time-temperature-transformation diagrams. Apart from the stability of various inclusions in a given composition of steel, the diagrams provide important kinetic information of diffusion controlled growth and dissolution.

Acknowledgment

The present study was supported by Division of Materials Sciences, Office of Basic Energy Sciences, the US Department of Energy under the grant DE-FG02-84ER45158.

References

1. S. S. Babu, S. A. David, J. M. Vitek, K. Mundra, and T. DebRoy, Mater. Sci. Technol. 11, 186 (1995).
2. S. S. Babu, S. A. David, and T. DebRoy, Sci. Technol. Welding Joining. 1, 17 (1996).

3. F. D. Richardson, Physical Chemistry of Melts in Metallurgy, vol. 2, p. 413, Academic Press, London (1974).
4. T. Hong, W. Pitscheneder, and T. DebRoy, Sci. Technol. Welding Joining. 2, 1 (1997).
5. J. W. Christian, The Theory of Transformations in Metals and Alloys, Part I: Equilibrium and General Kinetic Theory, 2nd ed., Pergamon Press, Oxford (1981).
6. M. J. Whelan, Met. Sci. J. 3, 95 (1969).
7. E. T. Turkdogan, Physical Chemistry of High Temperature Technology, Academic Press, New York (1980).
8. G. K. Sigworth and J. F. Elliott, Met. Sci. J. 8, 298 (1974).
9. G. H. Geiger and D. R. Poirier, Transport Phenomena in Metallurgy, p. 458, Addison-Wesley Publishing Company, Reading, MA.
10. O. Kluken and O. Grong, Metall. Trans. A. 20A, 1335 (1989).
11. K. C. Hsieh, S. S. Babu, J. M. Vitek, and S. A. David, Mater. Sci. Eng. A215, 84 (1996).
12. J. M. Dowling, J. M. Corbett, and H. W. Kerr, Metall. Trans. A. 17A, 1611 (1986).